Editors' Suggestion

Experimental realization of atomically flat and AlO_2-terminated $LaAlO_3$ (001) substrate surfaces

Jeong Rae Kim,[1,2] Jiyeon N. Lee,[3] Junsik Mun,[1,4] Yoonkoo Kim,[1,4] Yeong Jae Shin,[1,2] Bongju Kim,[1,2] Saikat Das,[1,2] Lingfei Wang,[1,2,*] Miyoung Kim,[1,4] Mikk Lippmaa,[3] Tae Heon Kim,[5,†] and Tae Won Noh[1,2]

[1]*Center for Correlated Electron Systems, Institute for Basic Science, Seoul 08826, Republic of Korea*

[2]*Department of Physics and Astronomy, Seoul National University, Seoul 08826, Republic of Korea*

[3]*Institute for Solid State Physics, University of Tokyo, Kashiwa 277-8581, Japan*

[4]*Department of Materials Science and Engineering and Research Institute of Advanced Materials, Seoul National University, Seoul 08826, Republic of Korea*

[5]*Department of Physics, University of Ulsan, Ulsan 44610, Republic of Korea*

(Received 30 August 2018; published 8 February 2019)

Oxide single-crystal substrates with atomically smooth and chemically uniform surfaces are indispensable for constructing sharp epitaxial heterointerfaces and investigating emergent interfacial physical phenomena. Here, we report a simple method to realize atomically flat and AlO_2-terminated $LaAlO_3$ (001) [LAO(001)] substrate surfaces. So far, the LAO(001) substrate has been utilized as a structural template for the epitaxial growth of a variety of oxide films. However, well-established methods for achieving atomically flat, singly terminated LAO(001) surfaces have rarely been reported. This is mainly due to the unstable charged surfaces of LaO^+ or AlO_2^-, which hinders simultaneous stabilizations of atomic-scale smoothness and single termination. To overcome this problem, we combined thermal annealing and subsequent deionized water leaching to treat the LAO(001) surface. We used atomic force microscopy to investigate the evolution of the LAO(001) surface during the water leaching and confirmed the atomically flat surface of the 120-min-water-leached sample. We further demonstrated the uniform AlO_2 termination of the LAO(001) surface via coaxial impact-collision ion scattering spectroscopy. Using the treated substrates, we are able to grow perovskite oxide films (i.e., $SrRuO_3$) on the LAO(001) substrate with atomically sharp heterointerfaces. Our paper provides an effective means for controlling the surface and interface of transition-metal oxide heterostructures at the atomic scale.

DOI: 10.1103/PhysRevMaterials.3.023801

I. INTRODUCTION

A variety of intriguing physics and highly tunable functionalities was discovered at the interfaces of perovskite oxide heterostructures during the last two decades [1,2]. In these active research fields based on complex oxide heterostructures, precise control of interfacial structure on an atomic level is of great importance. Specifically, by artificially manipulating the atomic termination sequence, we can stabilize and tune interfacial structure and associated physical phenomena which do not exist in bulk compounds. Fascinating examples include two-dimensional electron gas at a $LaAlO_3/SrTiO_3$ heterointerface [3], surface termination dependent electronic properties of $LaNiO_3$ ultrathin films [4], interfacial control of ferroelectricity and tunneling conductance in ultrathin ferroelectric films [5–7], and interface dipole engineering of the Schottky barrier [8].

Oxide heterostructures are usually grown epitaxially on single-crystal substrates. Hence, an atomically flat, singly terminated substrate surface is indispensable for realizing sharp heterointerfaces. Such surfaces were first realized on $SrTiO_3$ (001) substrates. $SrTiO_3$ has a cubic perovskite structure with nominally nonpolar SrO and TiO_2 layers alternating along the [001] crystallographic direction. Thanks to the distinct solubility of SrO and TiO_2 layers in acid, a uniformly TiO_2-terminated surface can be prepared via etching the $SrTiO_3$ substrate in buffered hydrofluoric acid [9,10]. Subsequent thermal annealing forms a simple step-terrace structure with atomic-level roughness [11]. Therefore, atomically flat $SrTiO_3$ substrates have been widely used to fabricate various complex oxide heterostructures.

$LaAlO_3$ (LAO) single crystal is another commonly used perovskite substrate for oxide thin-film growth. LAO has a smaller pseudocubic lattice constant (3.789 Å) than those of most perovskite-structured transition-metal oxides. This feature makes LAO an ideal template for strain engineering [12]. For instance, tetragonal-phase $BiFeO_3$ can be epitaxially stabilized on an LAO(001) substrate with a compressive strain [13]. The huge compressive strain between the film and the substrate ($\sim -4.5\%$) gives rise to the large tetragonality and enhanced ferroelectric polarization. In addition, unlike $SrTiO_3$ (001), the LAO(001) substrate has polar surfaces of LaO^+ or AlO_2^-. The polar surface can serve as an electrostatic boundary condition and tune the electronic properties of epitaxial films [14,15].

Despite such diverse use in oxide heterostructures, it is quite challenging to prepare an atomically flat and singly terminated LAO(001) surface. LAO can be conceptually viewed as a stack of alternating LaO^+ and AlO_2^- layers along the pseudocubic [001] direction. The polar nature of

*lingfei.wang@outlook.com
†thkim79@ulsan.ac.kr

these layers makes the structure unstable due to the diverging Coulomb energy cost. Therefore, the ideal LAO(001) surface can easily reconstruct either structurally or electronically in high temperature. It has already been demonstrated experimentally that the conventional methods of postannealing a chemically treated LAO(001) substrate can easily result in a mixed LaO and AlO_2 termination [16]. During the high-temperature (>930 °C) annealing process, a $\sqrt{5} \times \sqrt{5}$ La_4O_5 surface reconstruction can also occur, which impedes the formation of singly AlO_2-terminated LAO(001) surfaces [16,17].

In this paper, we describe a method to prepare atomically flat and AlO_2-terminated LAO(001) substrates. The method consists of high-temperature thermal annealing and subsequent deionized water leaching processes. The evolutions of the surface morphology with respect to the annealing conditions and leaching times were visualized using atomic force microscopy (AFM). We found that the LaO component at the LAO(001) surface can be gradually dissolved in water. Using coaxial impact-collision ion scattering spectroscopy (CAICISS), we confirmed that the final LAO(001) surface is uniformly terminated with an AlO_2 layer. The AlO_2-terminated surface is highly stable, even at high temperature up to 700°C. Using its robust surface stability, we demonstrate that we can epitaxially grow other complex oxide films with an atomically sharp heterointerface.

II. EXPERIMENTS

We used commercial LAO(001) single-crystal substrates (Crystec GmbH) with a miscut angle of less than 0.1°. We prepared the atomically flat LAO(001) surface by thermal annealing and deionized water leaching. During the thermal annealing, LAO substrates were kept in a tube furnace under flowing oxygen with a fixed flow rate of 0.5 L/min. The annealing was performed at 1000, 1100, or 1200°C for 3 h. The annealed LAO substrates were then dipped in deionized water and sonicated for a particular time duration (t_w) at room temperature (25 °C). For the sonication process, we used a 100-mL glass beaker (DURAN) and filled it with 50 mL deionized water. After the deionized water leaching process, the surface was sequentially rinsed with deionized water, ethanol, and acetone for 10 s each, in order to remove the chemical residuals generated during water leaching. We characterized the prepared LAO(001) surfaces using AFM (Cypher, Asylum Research) in ambient conditions. The spring constant, resonance frequency, and tip radius of the AFM tip (Tap300Al-G, Budget Sensors) are ~40 N/m, ~300 kHz, and <10 nm, respectively.

We carried out CAICISS measurements on the treated LAO(001) substrates at room temperature in an ultrahigh-vacuum chamber equipped with a CAICISS (TALIS-9700, Shimadzu) analyzer and a 2-keV He ion source. CAICISS is a form of low-energy ion scattering spectroscopy where the flight time of He ions backscattered from a crystal surface is measured [18]. Since the flight time depends on the energy lost in He ion collisions with surface atoms, peaks in a CAICISS time-of-flight (TOF) spectrum correspond to surface atom species with different atomic masses. Due to atomic shadowing effects, the peak intensities depend on the abundance of a particular atomic species at the surface as seen by the He ion beam in a particular incident direction relative to the crystal axes. CAICISS can thus be used to analyze both the chemical composition and structure of a crystal surface layer. During the CAICISS measurements, the background gas pressure was kept at $\sim 10^{-9}$ Torr. The ion scattering spectra were taken along the LAO[111] direction to identify the terminating layer of the crystals [19]. The [111] direction of the crystals was identified by taking in-plane azimuthal and out-of-plane polar angle scans of the He backscattering intensity and finding the symmetry point [20]. For an ideal perovskite structure, this would occur at an azimuthal angle of 45° (along the in-plane [110] azimuth) and a polar angle of 35° from the crystal surface plane.

We grew $SrRuO_3$ (SRO) epitaxial film on atomically flat LAO(001) substrates using pulsed laser deposition (PLD). A polycrystalline SRO target was ablated with a KrF excimer laser at an energy density of 1.5 J/cm^2 and a repetition rate of 3 Hz. During film growth, the LAO substrate temperature and oxygen pressure were maintained at 700 °C and 100 mTorr, respectively. The interfacial atomic configurations of the SRO/LAO(001) heterostructures were characterized by a cross-sectional high-angle annular dark-field scanning transmission electron microscope (HAADF-STEM) along the zone axis of LAO [100]. Atomic-resolution HAADF-STEM images were acquired using a spherical aberration-corrected JEM-ARM 200F (Cold FEG, JEOL Ltd, Japan). The analysis was conducted at an acceleration voltage of 80 kV to reduce the knock-on damage on SRO by the electron beam.

III. RESULTS AND DISCUSSION

A. Surface evolutions of LAO(001) substrates during thermal annealing

First, we investigated the LAO(001) surface evolution under various thermal annealing conditions. We used AFM in tapping mode for the surface topography studies. Figure 1(a) shows the AFM topography of an as-received LAO(001) crystal surface. Note that the surface of the as-received LAO(001) substrate is rough and we cannot see step-terrace structures. Figures 1(b)–1(d) show that systematic changes occur during the thermal treatment process. Here, the as-received LAO(001) substrates were annealed at 1000 °C [Fig. 1(b)], 1100 °C [Fig. 1(c)], and 1200 °C [Fig. 1(d)] for 3 h in oxygen flow. As the substrate annealing temperature increases, the surface atoms rearrange through diffusion, leading to the formation of sharp step edges over time. In general, the surface smoothness improved, and eventually a well-ordered step-terrace structure formed at 1200 °C. These experiments show that high-temperature thermal annealing is useful for forming an atomically flat step-terrace structure on an LAO(001) surface.

To examine the detailed surface termination state in the annealed LAO(001) substrates, we performed AFM phase-imaging analysis. Figures 1(e)–1(h) show the AFM phase images recorded simultaneously with the topography image during the AFM measurement. In the AFM phase images, a subtle change in the phase can arise from variation in the chemical composition on the sample surface [21]. Using

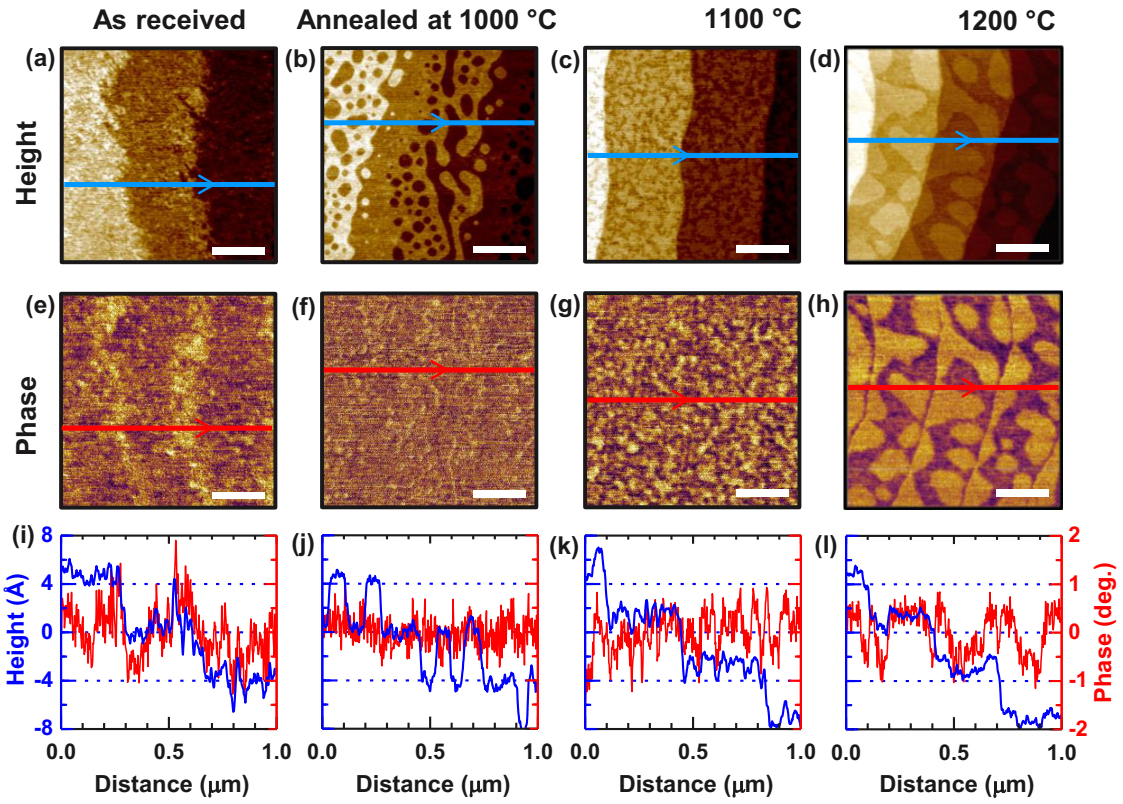

FIG. 1. Surface topography evolution of single crystal $LaAlO_3$ (001) under various thermal annealing conditions. Atomic force microscopy height [phase] images measured from (a) [(e)] as-received LAO(001) and from LAO(001) after annealing at (b) [(f)] 1000 °C, (c) [(g)] 1100 °C, and (d) [(h)] 1200 °C for 3 h in oxygen flow. The white scale bars in (a)–(h) are 250 nm long. All images have dimensions 1 × 1 μm. (i)–(l) Line profiles of the height and phase along, respectively, the blue and red lines in (a)–(d) and (e)–(h).

the phase contrast, we can identify spatial differences in the surface termination of an LAO(001) substrate [22,23]. For the as-received LAO(001) substrate surface with a mixed termination (i.e., LaO and AlO_2 layers), the spatial distribution of the phase is highly inhomogeneous. The terrace-edge regions exhibit much higher phase than those of the flat terrace regions. After annealing at 1000 °C, the inhomogeneity in the AFM phase decreases significantly, and the AFM phase image becomes more uniform. Interestingly, after increasing the annealing temperature up to 1100 °C or higher, the AFM phase becomes highly inhomogeneous again. The phase images [Figs. 1(g) and 1(h)] show distinct contrasts for different areas even within one flat terrace.

Line profiles analysis in Figs. 1(i)–1(l) provides further insight into the evolution of surface termination with annealing temperature. Figure 1(j) shows both topographic and phase line profiles of LAO after thermal annealing at 1000 °C. Note that there is a peak-to-valley height variation of about 0.4 nm (the blue line) and only slight phase variations (the red line). This indicates that the 1000°C-annealed LAO(001) has a singly terminated surface within the resolution of AFM imaging. This result is consistent with earlier reports of AlO_2-terminated LAO(001) substrate surfaces via thermal annealing [24,25]. However, as shown in Fig. 1(b), there is strong meandering along the step edges and many holes in the terraces probably due to the low surface diffusion rate. This indicates that the atomically flat LAO(001) surface with straight step edges cannot be obtained after 1000°C annealing.

We cannot obtain a singly terminated surface of the LAO(001) substrate by simply increasing the annealing temperature. Figure 1(l) shows the topographic (phase) profiles for the 1200°C-annealed sample along the lines marked in Fig. 1(d) [Fig. 1(h)]. Although well-arranged step-terrace-like features are visible, both the height and phase are highly inhomogeneous within each terrace. Note that the peak-to-valley height difference corresponds to half a unit cell. The LaO and AlO_2 sublayers are alternately stacked in LAO(001) and the presence of half-unit-cell height differences demonstrates that the surface terminations in the bright and dark regions must be different. It is probable that surface reconstruction, cation segregation, or the intermixing of La and Al atoms near the surface occur, driven by the entropy during high-temperature annealing [16,26]. This would lead to a nonuniform surface termination. Unlike the as-received substrate, the segregation of the two different surface terminations is in the scale of several hundred nanometers. This surface evolution after high-temperature annealing was constantly observed irrespective of the pretreatment method (e.g., acid etching), which is consistent with the earlier study [16]. Accordingly, additional steps after thermal annealing should be developed to obtain an atomically flat and singly terminated LAO(001) surface.

B. Deionized water leaching process for preparing atomically flat, singly terminated LAO(001) surfaces

In order to achieve an ideal LAO(001) surface for film growth, we developed a substrate preparation recipe. We reversed the conventional substrate preparation method consisting of chemical treatment and following postannealing. Namely, we start with preannealing LAO(001) at 1200°C to construct a step-terrace structure on an LAO(001) substrate surface. We then use a deionized water leaching process to obtain a single surface termination. Deionized water leaching has already been shown to be effective in controlling the surface termination of perovskite oxides such as $SrTiO_3$ (001) [27] and $BaSnO_3$ (001) [28]. In our case, during the water leaching process, the LaO layer on the LAO(001) surface may react with water and form water-soluble $La(OH)_3$ [29]. Then the deionized water may act as an etchant for $La(OH)_3$ and consequently remove the LaO surface layer.

The t_w-dependent evolution of the surface morphology during the water leaching process was found to be rather complicated. Figure 2 shows the AFM images taken after the water leaching process for each t_w. More detailed evolution is shown in Fig. S1 in the Supplemental Material [30]. Note that all topography images display a well-defined step-terrace structure produced by the preannealing process. Before water leaching ($t_w = 0$ min), the AFM images of the 1200 °C-annealed LAO(001) substrate are shown in Fig. 2(a), and the line profiles of height and phase are shown in Fig. 2(e). Consistent with the results shown in Figs. 1(d), 1(h), and 1(l), the AFM images exhibit well-defined step terraces but highly inhomogeneous phase. Surprisingly, as shown in Figs. 2(b) and 2(f), deionized water leaching for a short duration ($t_w =$ 1 min) can produce an atomically flat surface with a step-terrace structure. Nevertheless, as shown later, this surface is not suitable for practical film growth due to the poor stability in high temperature and moisture. Further increasing the deionized water leaching duration ($t_w > 1$ min), as shown in Fig. 2(i), makes the surface rougher at first but smoother at the end ($t_w > 120$ min). As shown in Figs. 2(c) and 2(g), the LAO(001) surface after water leaching for $t_w = 60$ min becomes rough with a mixed termination. In contrast, when $t_w \geqslant$ 120 min, the LAO(001) surface again becomes homogeneous and atomically flat. As shown in Fig. 2(d), the step-terrace morphology of the water leached LAO(001) substrate ($t_w =$ 120 min) is very sharp and there is no phase contrast [inset of Fig. 2(d)]. In the corresponding height and phase profiles [Fig. 2(h)], steps are one unit cell high and the phase shows negligible contrast. For even longer $t_w > 120$ min, the surface termination and roughness do not show notable changes (Fig. S1 in the Supplemental Material [30]). The t_w-dependent

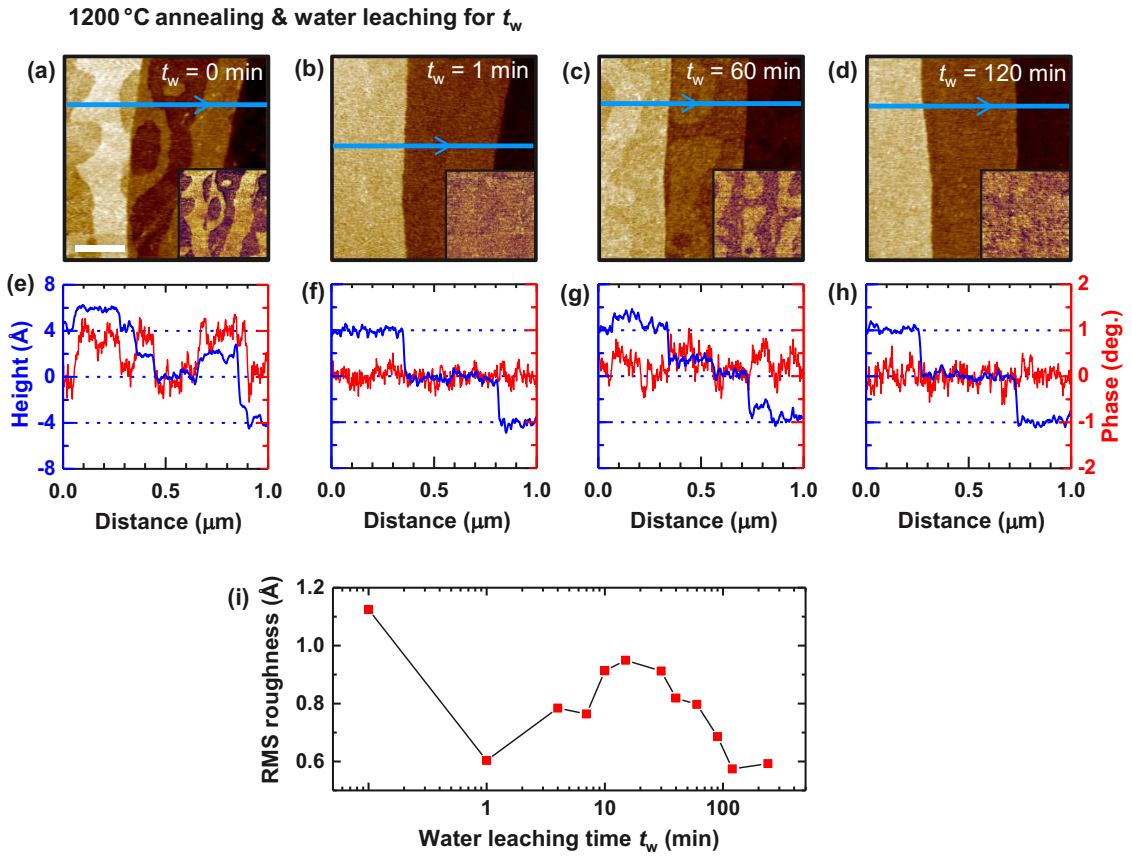

FIG. 2. Surface topography evolution of annealed LAO(001) surfaces during deionized water leaching. (a)–(d) AFM height images of annealed (1200 °C for 3 h in oxygen flow) LAO(001) single crystal after ultrasonic agitation in deionized water for leaching times $t_w = 0$, 1, 60, and 120 min. The white scale bar in (a) is 250 nm long. All images have dimensions 1 × 1 μm. The inset in (a)–(d) shows the corresponding phase images. (e)–(h) Line profile of height and phase along the blue lines in (a)–(d). (i) t_w-dependent surface roughness of LAO(001) surfaces.

evolution in Fig. 2 implies that we can obtain a stable and singly terminated LAO(001) surface with preannealing at 1200°C and following deionized water treatments for longer than 2 h.

C. Surface termination analysis by CAICISS

We performed CAICISS analysis to determine quantitatively the chemical compositions of the terminating layers in the water leached LAO(001) surfaces [18]. As shown in Fig. 3(a), when the He ion beam is aligned along the [111] direction of the LAO(001) substrate, only the cations of the topmost atomic layer can cause backscattering [19]. All the other cations in deeper layers are hidden due to the shadowing effect. Figure 3(b) shows the TOF spectra of scattered He ions, taken along the [111] crystal direction. The TOF spectra contain distinct scattering peaks for He collisions from La, Al, O, and C atoms at the LAO(001) surface. In addition to the signals from the directly backscattered He, there is a broad background associated with multiple scattering events. The backscattering peak intensities were obtained by Gaussian profile fitting (shown in blue, cyan) combined with a smoothly varying polynomial fitted to multiple scattering and background (shown in gray). The scattering peaks of lighter atoms tend to spread to longer flight times. We used two Gaussians (shown in red) for the oxygen peak fitting to account for the asymmetric peak shape. Since we focus on cations (La, Al), this oxygen peak fitting does not influence our analysis. The peak area was normalized by the theoretical scattering cross section for each element, which is approximately proportional to the square of the scattered atomic mass. The surface termination can then be analyzed by looking at the La:Al scattering intensity ratio.

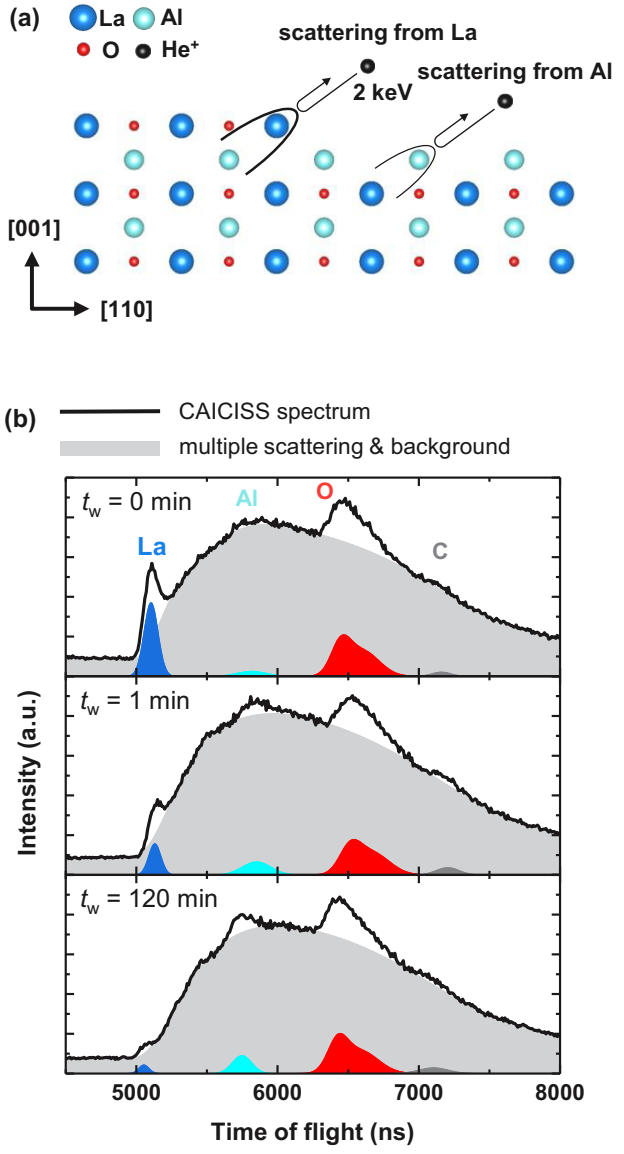

FIG. 3. CAICISS analysis of LAO(001) surfaces. (a) Schematic illustration of the CAICISS setup. (b) CAICISS spectrum of LAO(001) surfaces with $t_w = 0$, 1, and 120 min. The fitting peaks corresponding to La, Al, O, C, and multiple scattering are also included.

As shown in Fig. 3(b), the CAICISS peak intensities exhibit dramatic changes with t_w. In the case of the high-temperature-annealed but nonleached substrate ($t_w = 0$ min), the plot in Fig. 3(b) appears to show a large La scattering peak seemingly with a La:Al = 7:1 peak area ratio. Since the peak areas need to be normalized by scattering cross sections, the normalized La:Al ratio is 1:4. Assuming a perfect perovskite structure, about 20% of the surface appears to be terminated by the LaO layer and the remaining area is terminated by the AlO_2 layer. Note that this ratio may have some uncertainty due to the small intensity of the Al peak. Still, it does qualitatively confirm that a considerate amount of La is present on the surface. The La intensity dramatically decreases after the deionized water leaching process, while the Al peak intensity nearly triples for the $t_w = 120$-min sample. The normalized La:Al ratio is approximately 1:26 for the $t_w = 1$-min sample and 1:105 for the $t_w = 120$-min sample. We can thus conclude that the area of LaO-terminated regions significantly decreases during the water leaching, and the $t_w = 120$-min sample has a singly terminated AlO_2 surface. This result is consistent with the rapid dissolution of LaO species in water. More detailed analysis about CAICISS can be found in the Supplemental Material [30].

D. Possible surface structures of LAO(001) substrates after water leaching

We first focused on the nearly ideal AlO_2 surface termination after water leaching for $t_w > 120$ min. In fact, the realization of a perfect AlO_2 surface termination might be serendipitous. Note that a polar AlO_2^- surface without charge screening should be energetically unstable due to a polar catastrophe arising from the surface potential. Recently, it was theoretically predicted that the negative polarity of the surface AlO_2^- layer can be compensated by hydration or the formation of oxygen vacancies, which can stabilize uniform AlO_2 termination on LAO(001) surfaces [31]. Considering the fact that hydrated $Al(OH)_3$ is slightly soluble in water [32], an AlO_2-terminated LAO(001) surface would not be stable in the water leaching process for long duration ($t_w > 120$ min). Hence, it is more plausible that the AlO_2 surface termination layer in the LAO(001) substrate might be oxygen deficient,

that is, $AlO_{2-\delta}$. However, determination of the oxygen vacancy density in the surface layer is quite difficult for any oxide material. Further investigations are highly desirable to determine the actual stoichiometry of the topmost atomic layer.

Second, we would like to discuss the atomic structure of the LAO(001) surface after water leaching for $t_w = 1$ min. It looks like a singly terminated surface. The AFM topography and phase images [Fig. 2(b)] suggest that the intriguing surface might be atomically flat with one-unit-cell-high steps. Namely, it is actually similar to the single homogeneous layer case with a nearly zero phase contrast. However, this surface is not stable during further water leaching. We tested the surface stability of the $t_w = 1$-min sample during the further thermal annealing process and compared it with the case of the $t_w = 120$-min sample. To mimic the typical growth condition of oxide heterostructures, the samples were annealed again at 700°C in a high vacuum (an oxygen partial pressure of 10^{-6} Torr) for 1 h. We found that the $t_w = 1$-min sample surface cannot remain atomically flat and singly terminated, while the $t_w = 120$-min sample surface remains intact (Fig. S2 in the Supplemental Material [30]). Furthermore, as shown in Fig. 2(c), the uniform termination of the $t_w = 1$-min surface degrades over several tens of minutes of continuous water leaching treatments. This result implies that the $t_w = 1$-min sample may change due to ambient humidity as well. Therefore, the $t_w = 1$-min LAO(001) substrate is not suitable for the practical growth of complex oxide films and heterostructures.

The CAICISS experiments also indicated that the $t_w = 1$-min LAO(001) surface has incomprehensive stoichiometry. They showed that the La:Al ratio is about 1:26, which means that the surface is Al rich. Based on the polar-angle-dependent CAICISS measurements discussed in the Supplemental Material, the crystallinity of the topmost unit-cell layer appears to be low (Fig. S3 in the Supplemental Material [30]). Possible mechanisms that can explain the AFM and CAICISS results include the presence of a particular surface reconstruction and, more likely, a layer with either La vacancy defects or La-Al antisite substitutions [26]. Further studies are required to understand the atomic-scale origin of this intermediate surface. The incomprehensive stoichiometry also makes it difficult to

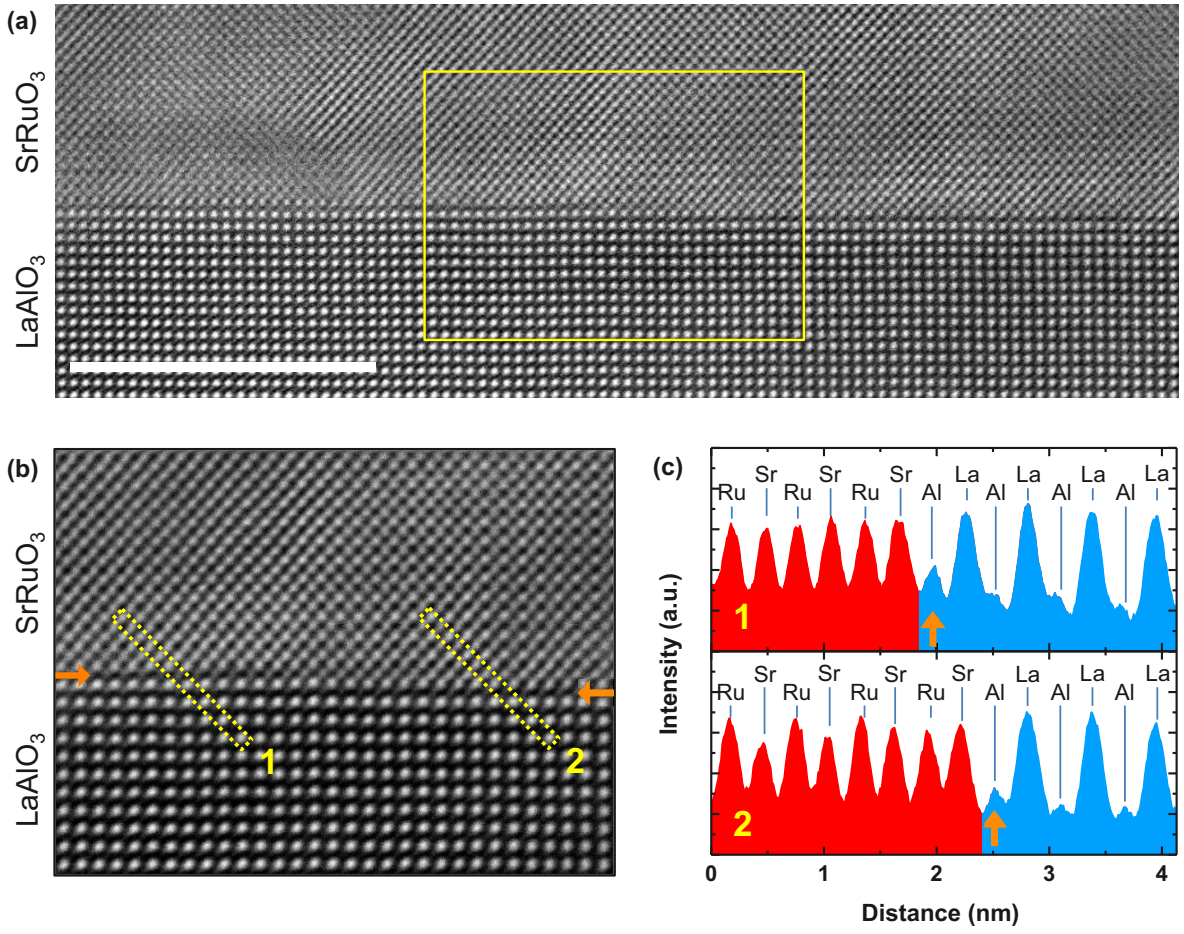

FIG. 4. Cross-sectional STEM analysis on $SrRuO_3$/LAO(001) interfaces. (a) HAADF-STEM image measured along the [100] zone axis of LAO. The scale bar corresponds to 10 nm. (b) Zoomed-in HAADF-STEM image from the area marked by the solid box in (a). Both images show a sharp SrO-AlO_2-terminated interface and a one-unit-cell-high step. The interfaces in the left- and right-hand sides of (b) are marked by solid arrows. (c) Line profiles of HAADF-STEM intensity along the dashed boxes marked in (b).

use the t_w = 1-min LAO(001) substrate for practical oxide thin-film growth.

E. Heterointerfaces grown on AlO_2-terminated LAO(001) surfaces

The real impetus of our studies is to realize atomically sharp heterointerfaces with the AlO_2-terminated LAO(001). Based on this consideration, we tested the availability of the AlO_2-terminated LAO(001) substrate for the growth of oxide thin films. Here we grew a prototypical SRO film via PLD on the AlO_2-terminated LAO(001) substrate prepared by water leaching. We investigated the atomic termination sequence at the SRO/LAO(001) heterointerface with the STEM. As shown in Fig. 4(a), the HAADF image confirmed the uniform and atomically sharp SRO/LAO interface. In the magnified image in Fig. 4(b), more clear atomic configurations and step-terrace structures are visible. To determine the stacking sequence at the interface, we plotted the line profiles along the yellow dashed boxes in Fig. 4(b). The peak intensities of atoms (Sr, Ru, La, and Al) are determined by the atomic number. As shown in Fig. 4(c), the profile signifies a uniform interfacial stacking sequence of RuO_2-SrO-AlO_2-LaO. This result further demonstrates that the AlO_2-terminated LAO(001) prepared by water leaching is highly stable in the conventional deposition environment of complex oxide thin films. The physical adsorbates (e.g., water molecules, carbonates) that may occur during the water leaching process appear to be effectively removed during the high-temperature annealing (700°C) and film growth procedures. Therefore, this substrate preparation method can be practically applicable for achieving atomically sharp heterointerfaces on LAO(001) substrates.

IV. SUMMARY

In summary, we realized atomically flat, singly terminated LAO(001) surfaces via preannealing and subsequent deionized water leaching. Our method for treating LAO(001) substrates is simple and free of hazardous chemicals. We believe that this technique can be used to achieve better control over the surface or interface states in the heterostructures grown on LAO(001) substrates and thus facilitates the exploration of exotic phenomena at complex oxide heterointerfaces. Furthermore, our paper could serve as a guideline for manipulating surface terminations of various other polar oxide substrates with rare-earth atoms, such as $YAlO_3$, $NdGaO_3$, or yttria-stabilized zirconia.

ACKNOWLEDGMENTS

This work was supported by IBS-R009-D1. J.N.L. was supported by the Japan Society for the Promotion of Science (JSPS) Fellows and the Program for Leading Graduate Schools (MERIT). This paper was supported by JSPS Grants-in-Aid for Scientific Research (Grants No. 26105002 and No. 18J20046). STEM analysis was supported by the National Center for Inter-University Research Facilities at Seoul National University in Korea. T.H.K. acknowledges the National Research Foundation of Korea (NRF) grants funded by the Korea government (Ministry of Education) (Grant No. 2017R1D1A1B03028614) and the support of the NRF (Grant No. 2014R1A4A1071686). We thank J.-G. Yoon, J.-S. Chung, D. Lee, S. H. Chang, and S. M. Yang for valuable discussions and comments.

[1] H. Y. Hwang, Y. Iwasa, M. Kawasaki, B. Keimer, N. Nagaosa, and Y. Tokura, Nat. Mater. **11**, 103 (2012).
[2] P. Zubko, S. Gariglio, M. Gabay, P. Ghosez, and J.-M. Triscone, Annu. Rev. Condens. Matter Phys. **2**, 141 (2011).
[3] A. Ohtomo and H. Y. Hwang, Nature (London) **427**, 423 (2004).
[4] D. P. Kumah, A. Malashevich, A. S. Disa, D. A. Arena, F. J. Walker, S. Ismail-Beigi, and C. H. Ahn, Phys. Rev. Appl. **2**, 054004 (2014).
[5] P. Yu, W. Luo, D. Yi, J. X. Zhang, M. D. Rossell, C.-H. Yang, L. You, G. Singh-Bhalla, S. Y. Yang, Q. He, Q. M. Ramasse, R. Erni, L. W. Martin, Y. H. Chu, S. T. Pantelides, S. J. Pennycook, and R. Ramesh, Proc. Natl. Acad. Sci. USA **109**, 9710 (2012).
[6] Y. J. Shin, Y. Kim, S.-J. Kang, H.-H. Nahm, P. Murugavel, J. R. Kim, M. R. Cho, L. Wang, S. M. Yang, J.-G. Yoon, J.-S. Chung, M. Kim, H. Zhou, S. H. Chang, and T. W. Noh, Adv. Mater. **29**, 1602795 (2017).
[7] L. Wang, R. Kim, Y. Kim, C. H. Kim, S. Hwang, M. R. Cho, Y. J. Shin, S. Das, J. R. Kim, S. V. Kalinin, M. Kim, S. M. Yang, and T. W. Noh, Adv. Mater. **29**, 1702001 (2017).
[8] T. Yajima, Y. Hikita, and H. Y. Hwang, Nat. Mater. **10**, 198 (2011).
[9] M. Kawasaki, T. Maeda, R. Tsuchiya, and H. Koinuma, Science **266**, 1540 (1993).
[10] G. Koster, B. L. Kropman, G. J. H. M. Rijnders, D. H. A. Blank, and H. Rogalla, Appl. Phys. Lett. **73**, 2920 (1998).
[11] M. Lippmaa, M. Kawasaki, A. Ohtomo, T. Sato, M. Iwatsuki, and H. Koinuma, Appl. Surf. Sci. **130**, 582 (1998).
[12] D. G. Schlom, L.-Q. Chen, C.-B. Eom, K. M. Rabe, S. K. Streiffer, and J.-M. Triscone, Annu. Rev. Mater. Res. **37**, 589 (2007).
[13] D. Sando, A. Barthélémy, and M. Bibes, J. Phys. Condens. Matter **26**, 473201 (2014).
[14] M. Minohara, T. Tachikawa, Y. Nakanishi, Y. Hikita, L. F. Kourkoutis, J.-S. Lee, C.-C. Kao, M. Yoshita, H. Akiyama, C. Bell, and H. Y. Hwang, Nano. Lett. **14**, 6743 (2014).
[15] T. Higuchi, Y. Hotta, T. Susaki, A. Fujimori, and H. Y. Hwang, Phys. Rev. B **79**, 075415 (2009).
[16] A. J. H. van der Torren, S. J. van der Molen, and J. Aarts, Phys. Rev. B **91**, 245426 (2015).
[17] C. H. Lanier, J. M. Rondinelli, B. Deng, R. Kilaas, K. R. Poeppelmeier, and L. D. Marks, Phys. Rev. Lett. **98**, 086102 (2007).
[18] M. Katayama, E. Nomura, N. Kanekawa, H. Soejima, and M. Aono, Nucl. Instrum. Methods Phys. Res. B **33**, 857 (1988).
[19] T. Ohnishi, K. Takahashi, M. Nakamura, M. Kawasaki, M. Yoshimoto, and H. Koinuma, Appl. Phys. Lett. **74**, 2531 (1999).

[20] M. Yoshimoto, T. Maeda, K. Shimozono, H. Koinuma, M. Shinohara, O. Ishiyama, and F. Ohtani, Appl. Phys. Lett. **65**, 3197 (1994).
[21] R. García, R. Magerle, and R. Perez, Nat. Mater. **6**, 405 (2007).
[22] R. Bachelet, F. Sánchez, F. J. Palomares, C. Ocal, and J. Fontcuberta, Appl. Phys. Lett. **95**, 141915 (2009).
[23] R. Gunnarsson, A. S. Kalabukhov, and D. Winkler, Surf. Sci. **603**, 151 (2009).
[24] D.-W. Kim, D.-H. Kim, B.-S. Kang, T. W. Noh, D. R. Lee, and K.-B. Lee, Appl. Phys. Lett. **74**, 2176 (1999).
[25] Z. Q. Liu, Z. Huang, W. M. Lü, K. Gopinadhan, X. Wang, A. Annadi, T. Venkatesan, and Ariando, AIP Adv. **2**, 012147 (2012).
[26] X. Luo, B. Wang, and Y. Zheng, Phys. Rev. B **80**, 104115 (2009).
[27] J. G. Connell, B. J. Isaac, G. B. Ekanayake, D. R. Strachan, and S. S. A. Seo, Appl. Phys. Lett. **101**, 251607 (2012).
[28] W.-J. Lee, H. Lee, K.-T. Ko, J. Kang, H. J. Kim, T. Lee, J.-H. Park, and K. H. Kim, Appl. Phys. Lett. **111**, 231604 (2017).
[29] D. R. Lide, *CRC Handbook of Chemistry and Physics* (CRC, Boca Raton, FL, 2004).
[30] See Supplemental Material at http://link.aps.org/supplemental/10.1103/PhysRevMaterials.3.023801 for detailed evolution of LAO(001) surfaces during deionized water leaching, stability of t_w = 1-min and 120-min samples under thermal annealing, and CAICISS polar angle scan experiments.
[31] K. Krishnaswamy, C. E. Dreyer, A. Janotti, and C. G. Van de Walle, Phys. Rev. B **90**, 235436 (2014).
[32] K. H. Gayer, L. C. Thompson, and O. T. Zajicek, Can. J. Chem **36**, 1268 (1958).